

Energy gaps in Bi-Sr-Ca-Cu-O and Bi-Sr-Cu-O systems by electron tunneling

T. Ekino* and J. Akimitsu

Department of Physics, Aoyama-Gakuin University, 6-16-1 Chitosedai, Setagaya, Tokyo 157, Japan

(Received 9 December 1988; revised manuscript received 5 April 1989)

We report the results of electron tunneling studies of the Bi-Sr-Ca-Cu-O and Bi-Sr-Cu-O systems by using point-contact tunneling. In these studies, we observed two distinctive energy gaps at each Bi-Sr-Ca-Cu-O system, having extremely large values. The larger values of the ratios $2\Delta/kT_c$ are 10–12 for $\text{Bi}_2\text{Sr}_2\text{CaCu}_2\text{O}_y$, and 9–11 for $\text{Bi}_2\text{Sr}_2\text{Ca}_2\text{Cu}_3\text{O}_y$, and the smaller values are 5.5–6.1 for $\text{Bi}_2\text{Sr}_2\text{Ca}_2\text{Cu}_3\text{O}_y$. These differences can be attributed to the gap anisotropies and the ratios of gaps are 1.7–1.8 for $\text{Bi}_2\text{Sr}_2\text{CaCu}_2\text{O}_y$, and 1.5–1.8 for $\text{Bi}_2\text{Sr}_2\text{Ca}_2\text{Cu}_3\text{O}_y$. The ratio $2\Delta/kT_c$ in the Ca-absent material $\text{Bi}_2\text{Sr}_2\text{CuO}_y$ was obtained as 5.4–7.4. The gap values are quite reproducible for the bulk, single crystal, and thin films.

I. INTRODUCTION

Common characteristic features of high- T_c superconductivity have been associated with the existence of CuO_2 planes in their crystal structures. To understand the essential features of this superconductivity, various physical properties have been investigated by several experimental techniques. Among them, knowledge of the energy gaps is crucial for understanding the superconducting natures in these systems. Especially, electron tunneling is the most direct probe to measure the energy gaps. Several reports on tunneling measurements confirm that the ratios are $2\Delta/kT_c = 5$ for $\text{La}_{2-x}\text{Sr}_x\text{CuO}_y$ (La-Sr-Cu-O) and 3–5 for $\text{YBa}_2\text{Cu}_3\text{O}_y$ (Y-Ba-Cu-O).¹ However, in other studies, $2\Delta/kT_c = 6$ –11 are reported for Y-Ba-Cu-O.^{2,3} These differences can be attributed to (1) the anisotropy of gaps which is related to the directions parallel and perpendicular to the CuO_2 planes, and (2) the uncertainty of the methods for determining the energy gap 2Δ from the experimental data. For example, 2Δ is determined from the peak-to-peak value in tunnel conductance, or determined from the fitting with the assumed gap function, or from the bias difference where normal and superconducting tunnel conductances cross each other. Our results on La-Sr-Cu-O and Y-Ba-Cu-O yield $2\Delta/kT_c = 4$ –5,^{4,5} using the energy gaps by fitting the BCS density of states to the observed tunnel conductances.

In this paper, we report the measurements of extremely large gaps in Bi-Sr-Ca-Cu-O and large gaps in Ca absent Bi-Sr-Cu-O systems. Observed values of energy gaps in Bi-Sr-Ca-Cu-O are larger than those of Y-Ba-Cu-O, although the latter has nearly the same T_c as the former. To check the reproducibility of these large gap values, the measurements have been done by using the samples under several synthesis conditions. Anisotropies of gaps in Bi-Sr-Ca-Cu-O were also measured by using thin films. The results indicate that the gap anisotropies in Bi-Sr-Ca-Cu-O are larger than those of Y-Ba-Cu-O. This tendency is consistent with the critical-field measurements.⁶ As for Bi-Sr-Cu-O, the gap values are considerably larger than those of conventional strong-coupling superconductors, although its T_c is not so high.

II. SAMPLE PREPARATIONS

Samples used in the present experiments are polycrystals, single crystals, and sputtered films of Bi-Sr-Ca-Cu-O (Refs. 7,8) and polycrystals of Bi-Sr-Cu-O.^{9,10} Polycrystalline Bi-Sr-Ca-Cu-O samples were prepared by solid-state reactions. Mixtures of Bi_2O_3 , SrCO_3 , CaCO_3 , and CuO are pressed into pellets and fired. Our first sample (we refer to as *S*-1 hereafter) has the nominal compositions of Bi:Sr:Ca:Cu = 1:1:1:2, fired at 800 °C for 5 h and 880 °C for 12–20 h in air. Our single crystal (*S*-2) is nominally Bi:Sr:Ca:Cu = 1:2:2:4, cooled down from 980 °C to 800 °C at the rate of 2 °C/h in air. Our third sample (*S*-3) is Bi:Sr:Ca:Cu = 2:2:1:2, fired at 870 °C for 36 h under a flowing oxygen gas. A Pb doped sample Pb:Bi:Sr:Ca:Cu = 0.6:1.4:2:2:3 (*S*-4) was sintered at 845 °C for 240 h in air. Sputtered films (*S*-5) were kindly offered by Dr. Nakada of Aoyama-Gakuin University and their nominal composition was Pb:Bi:Sr:Ca:Cu = 0.2:2.0:2.1:1.7:3.0. Details are in Ref. 8. Polycrystalline Bi-Sr-Cu-O samples were synthesized in air as follows: Bi:Sr:Cu = 2.0:2.0:1.3 at 900 °C for 12–24 h (*S*-6) and 2:2:1 at 900 °C for 240 h (*S*-7). X-ray diffraction patterns of Bi-Sr-Ca-Cu-O samples showed a mixture of two phases, but did not have any additional peaks. The scanning electron microscope (SEM) images suggested that the repeated reaction and pulverization in the Bi-Sr-Ca-Cu-O sample made the grain sizes about an order of magnitude smaller. Large grain sizes are favorable for the tunneling measurements. Therefore, to make the larger grain sizes, starting materials of polycrystals were reacted carefully at one time. T_c 's were measured by the standard dc four-probe method, T_c 's (onset-midpoint-endpoint) are, 111–76 K double transitions for *S*-1, 88–84–76 K (*S*-2), 86–83–80 K (*S*-3), 113–110–108 K (*S*-4) [$\rho(300\text{ K}) = 2.8\text{ m}\Omega\text{ cm}$], 119–114–103 K (*S*-5) [$\rho(300\text{ K}) = 1.9\text{ m}\Omega\text{ cm}$], 8.0–7.1–6.5 K (*S*-6) [$\rho(300\text{ K}) = 17.9\text{ m}\Omega\text{ cm}$], 11–9–7 K (*S*-7). The transition widths $\Delta T_c(10\%–90\%)/T_c$ (end point) of Bi-Sr-Ca-Cu-O samples are within 9% and 4% at the narrowest transition temperature. However, in the Bi-Sr-Cu-O system, the transition widths are rather broad ($\Delta T_c/T_c = 10\%–30\%$). The sample *S*-7 became super-

conducting after long-term annealing and showed semi-conducting behavior above the transition temperature in the resistivity measurements. Meissner measurements showed the superconducting volume fraction of more than 60%–70% for Bi-Sr-Ca-Cu-O and less than 10%–20% for Bi-Sr-Cu-O.

III. TUNNELING MEASUREMENTS

Electron tunneling was measured by a point-contact configuration with Al or Pt sheets.¹¹ The Al sheet was polished with electrolysis and was oxidized on its surface. Cleaved and edged surfaces of samples came in contact mechanically with an Al or Pt surface. In order to avoid the effect of the contact resistance at the electrodes, the four-probe method was employed for each measurement. Au conducting paste was used to attach the electrodes. Tunnel junction areas are 0.1–1.0 mm². For the thin-film measurements, Al sheets were used for the measurements of tunneling parallel to CuO₂ planes, and Al needles were used for tunneling perpendicular to CuO₂ planes. Dynamic conductances dI/dV , where I and V are the tunnel current and the dc bias voltage, respectively, were measured by an ac modulation method with a modulation amplitude of 250–500 μ V for Bi-Sr-Ca-Cu-O and 50–200 μ V for Bi-Sr-Cu-O. Bias voltage sweeps took 1–2 min across the peaks in the dI/dV curves. The detector of the modulated tunnel currents was the PAR-MODEL-124A Lock-In Amplifier with a 116 preamplifier. Time constants were less than 1 ms in each measurement. Temperatures were raised by 1–2 K per h.

IV. EXPERIMENTAL RESULTS

A. Gap measurements in Bi-Sr-Ca-Cu-O systems

Figures 1(a) and 2(a) show the I - V and dI/dV - V curves in sample S -1 for Bi₂Sr₂Ca₁Cu₂O _{y} (Bi-Sr-Ca-Cu-O 2:2:1:2) phase and Bi₂Sr₂Ca₂Cu₃O _{y} (Bi-Sr-Ca-Cu-O 2:2:2:3) phase, respectively. Tunnel resistances at higher-bias regions are about 10 k Ω and 5 k Ω , respectively. Flat background conductances against the biases and the symmetric dI/dV curves with respect to zero bias were often observed, which were hardly observed in the cases of La-Sr-Cu-O and Y-Ba-Cu-O.

To determine the energy-gap values, we tried to analyze the data on the basis of the BCS theory. The BCS density of states at $T=0$ K yields the expression

$$RI(V) = (V^2 - \Delta^2)^{1/2}, \quad (1)$$

where R is the tunnel resistance at the higher-bias region.¹² Figures 1(b) and 2(b) show the V^2 versus I^2 plots. V at $I=0$ gives Δ , and $2\Delta=81$ and 92 meV were obtained for each case. A similar method was employed by Hawley *et al.* in organic and high- T_c superconductors.^{13,14} Next, we determined the gap values from the observed dI/dV curves. In these cases, we tried to fit the broadened BCS density of states $D(E, \Gamma)$ proposed by Dynes *et al.*¹⁵ to the observed dI/dV curves, where

$$D(E, \Gamma) = \text{Re}\{(E - i\Gamma)/[(E - i\Gamma)^2 - \Delta^2]^{1/2}\} \quad (2)$$

and Γ is the broadening parameter. The temperature factor was considered for the fitting calculations. It should be emphasized that the peak-to-peak values in dI/dV at finite temperatures are, in our opinion, over estimated and should not be adopted as the energy gaps. Figures 1(c) and 1(d) present the fitting results at $T=6.0$ and 57.6 K. Solid circles are the experimental data normalized by the background conductances. Data points in Fig. 1(c) are taken from the dI/dV curve in Fig. 1(a), where the background conductance is also shown by the broken line. The results give $2\Delta=76.0$ meV and $\Gamma=13.3$ meV for Fig. 1(c) and $2\Delta=60.4$ meV and $\Gamma=17.0$ meV for Fig. 1(d). At low temperatures, the gap values are also given by the interval of points where the superconducting conductance $(dI/dV)_s$ and background (normal) conductance $(dI/dV)_n$ crosses each other [$(dI/dV)_s = (dI/dV)_n$]. This method yields $2\Delta=81$ meV in Fig. 1(a). The gap values determined with these methods are almost consistent with each other. In these experiments, we also pay special attention to determining T_c . T_c determined from the tunnel junction is more reliable than that obtained from zero resistance or Meissner measurements. Figure 3 shows the temperature dependence of dI/dV (0 mV) normalized to dI/dV (140 mV) in Fig. 2(a). From the temperature that dI/dV (0 mV) begins to reduce, T_c is assigned as about 105 K. Using the T_c 's determined from this method, the ratios $2\Delta/kT_c$ for Bi-Sr-Ca-Cu-O 2:2:1:2 and Bi-Sr-Ca-Cu-O 2:2:2:3 are 11.6–12.4 and 10.0–11.0, respectively. These are consistent with the results of reference 16. Temperature dependences of energy gaps are shown in Fig. 4. 2Δ 's were determined by using the fitting procedure described above. The gap values are well above their BCS values, but their temperature variations coincide with the scaled BCS curves. To check the reproducibility of these extremely large gap values, we prepared the samples under several synthesis conditions. Tunneling parallel to the CuO₂ planes has been measured on the single crystal (S -2). Figure 5 shows the I - V and dI/dV - V curves. 2Δ is about 73 meV from $(dI/dV)_s = (dI/dV)_n$, the value $2\Delta/kT_c$ is 9.6–11.0, almost the same as the Bi-Sr-Ca-Cu-O 2:2:1:2 phase in S -1. Figure 6(a) shows the temperature variation of dI/dV curves from sample S -3. Very sharp gap structures were observed at around $T=60$ K. The reduction of $(dI/dV)_s/(dI/dV)_n$ begins at $V=120$ mV, outside the gap. Tunnel resistances at $T=52.9$ K are 1.7 k Ω at $V=40$ mV and 3.7 k Ω near zero bias. The $(dI/dV)_n$ increases against bias voltages and fairly symmetrical with respect to the Fermi level. As is shown in Fig. 6(a), peaks in dI/dV curves are gradually smeared when the temperatures are raised, but the peak positions in dI/dV curves do not shift to lower biases. The peak positions in dI/dV shift to rather higher biases with thermal broadening and are smeared out at about $T=100$ K. 2Δ at $T=52.9$ K is about 60 meV determined from $(dI/dV)_s = (dI/dV)_n$ and about 50 meV from an I^2 versus V^2 plot. This gap value at $T=0$ K is about 6% larger than that at $T=52.9$ K assuming that the temperature dependence of the energy gap obeys the BCS curve. The small energy gap in Fig. 6(a) compared to that in Fig. 2(a) can be attributed to the gap anisotropies. This will be discussed later. Figure

6(b) shows the temperature variation of dI/dV (0 mV) normalized by dI/dV (100 mV). Data corresponds to that in Fig. 6(a), indicating that the main phase at point contact regions is the Bi-Sr-Ca-Cu 2:2:2:3 compound, although Josephson-like anomalies at zero biases are also observed up to $T=73$ K, the vicinity of the zero-

resistance temperature $T=79$ K. The reduction of dI/dV (0 mV) are observed up to 104 K, thus the ratio $2\Delta(T=0 \text{ K})/kT_c$ is 5.9–7.1. To measure the energy gap of Bi-Sr-Ca-Cu 2:2:2:3 phase more precisely, we have synthesized the Pb doped Bi-Sr-Ca-Cu 2:2:2:3 phase (sample S-4). Figure 7(a) shows the $I-V$ and $dI/dV-V$ curves

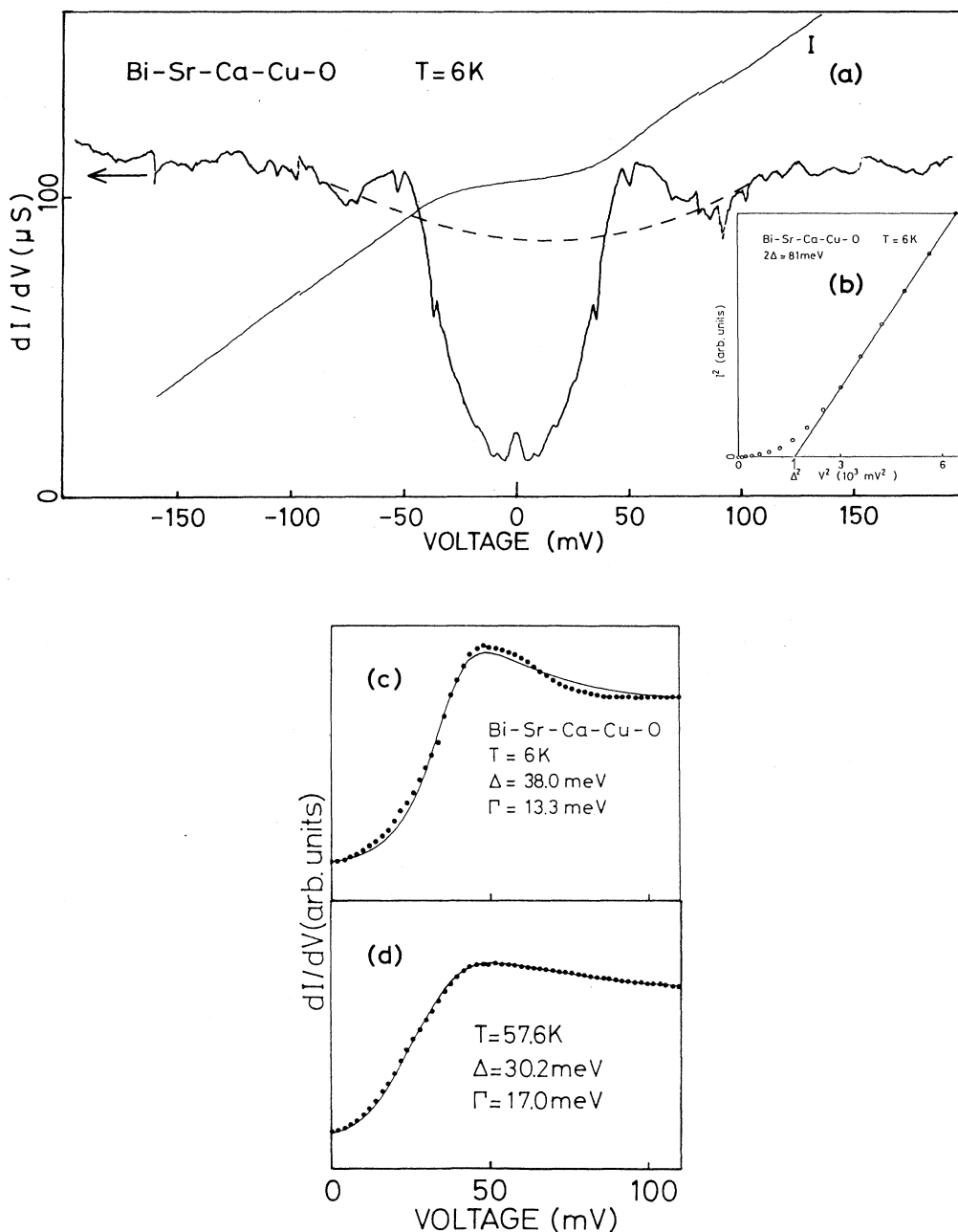


FIG. 1. (a) The $I-V$ and $dI/dV-V$ curves of Bi-Sr-Ca-Cu-O 2:2:1:2 phase in sample S-1. The broken line is the background conductance $(dI/dV)_n$ interpolated from higher-bias regions. (b) The I^2 vs V^2 plot taken from the $I-V$ curve in Fig. 1(a). (c) and (d) Fitting results of the $D(E, \Gamma)$ to the experimental data at (c) $T=6.0$ K and (d) $T=57.6$ K. Solid lines show the $D(E, \Gamma)$ with temperature broadening. Solid circles are the experimental data normalized by the background conductance $(dI/dV)_n$. Experimental data in (c) are taken from the dI/dV curve in (a).

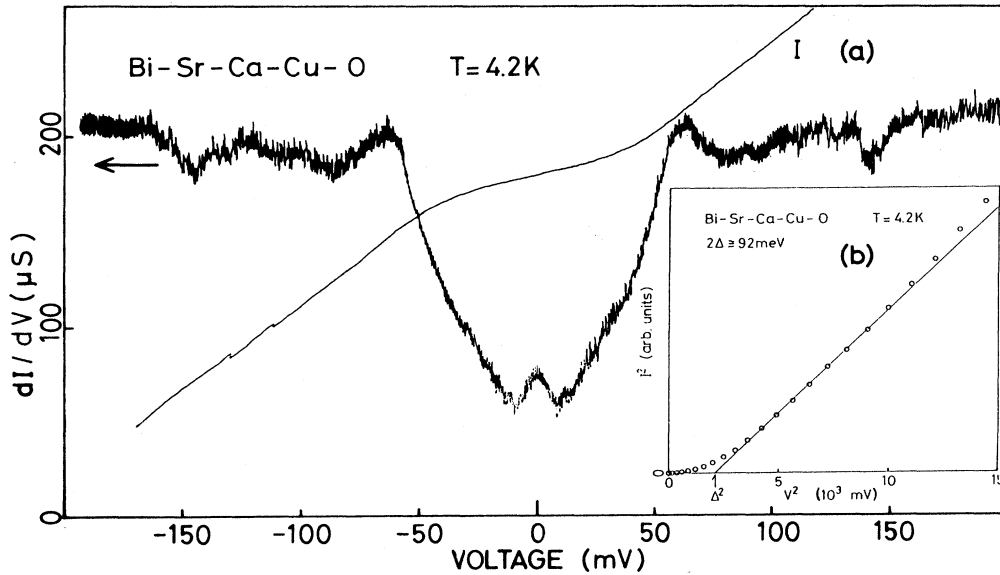


FIG. 2. (a) The I - V and dI/dV - V curves of Bi-Sr-Ca-Cu-O 2:2:2:3 phase in sample S-1. (b) The I^2 vs V^2 plot taken from the I - V curve in (a).

from S-4. The gap structure is clearly observed. The absence of anomaly in dI/dV (0 mV) suggests the absence of short circuits in the tunnel junction and dI/dV (0 mV) is well reduced by about 90% of its peaks in dI/dV . A plot of I^2 versus V^2 [Fig. 7(b)] gives $2\Delta = 85$ – 87 meV from the straight line fitting and this almost coincides with the gap value determined from the third procedure described above [$(dI/dV)_s = (dI/dV)_n$]. Figure 7(c) shows the raw data of dI/dV at different temperatures taken from the same junction in Fig. 7(a). Since the tunnel junction became unstable at about $T = 60$ K, the measurements up to T_c could not be succeeded. In Figs. 7(a) and 7(c), negative peaks in dI/dV exist at around $V = 90$ mV and reductions in dI/dV outside of their peaks begin at about $V = 120$ mV. These phenomena are observed also in Figs. 1(a) and 6(a) and are also reported in reference 17.

B. Gap anisotropies in Bi-Sr-Ca-Cu-O systems

The energy gaps in Bi-Sr-Ca-Cu-O are expected to have large anisotropies with respect to being perpendicu-

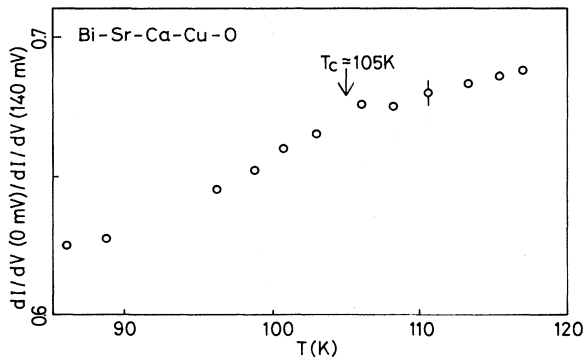


FIG. 3. Temperature variation of the dI/dV at zero bias normalized by the dI/dV at bias of 140 mV. The gap is opening at $T = 105$ K. The sample is S-1.

lar and parallel to CuO_2 planes. For example, Iye *et al.*⁶ reported that $H_{c2}(\parallel\text{CuO}_2)/H_{c2}(\perp\text{CuO}_2) = 10$ – 60 in Bi-Sr-Ca-Cu-O, 2:2:1:2 where $\parallel\text{CuO}_2$ and $\perp\text{CuO}_2$ mean parallel and perpendicular to the CuO_2 planes. The value is larger than that of Y-Ba-Cu-O.^{4–7} We show the results of gap anisotropy measurements by using the oriented films (S-5). Figure 8(a) shows the dI/dV - V curves from point contact tunnel junctions of Bi-Sr-Ca-Cu-O 2:2:2:3 perpendicular ($\perp\text{CuO}_2$) and parallel ($\parallel\text{CuO}_2$) to the CuO_2 planes. In the process of measuring of films, we observed single gap structures at the first contact, but after the repeated adjustments of contact conditions additional gap structures can be observed. These facts suggest that the frequent readjustments distort the sample surface because the sample is pressed into the counter electrode, or a needle penetrates the sample and the electrons from several directions of crystal axes are detected.

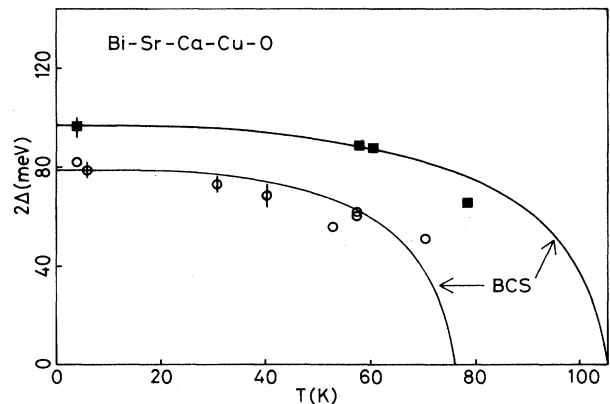


FIG. 4. Temperature dependences of the energy gaps for Bi-Sr-Ca-Cu-O (sample S-1). 2Δ are extracted by using Eq. (2). Open circles and solid squares correspond to Bi-Sr-Ca-Cu-O 2:2:1:2 and Bi-Sr-Ca-Cu-O 2:2:2:3 phases, respectively.

Thus, it raises the question that we are actually measuring the anisotropies of the energy gaps in these samples. However, we obtained the strong relationship ($>60\%$ – 70%) between the gap values and the directions of the CuO_2 planes at the interfaces of the tunnel junctions. Therefore, we concluded that two different gap values correspond to those of different crystalline directions, i.e., $\perp\text{CuO}_2$ and $\parallel\text{CuO}_2$, respectively. The observed values are $2\Delta(\perp\text{CuO}_2)=49\text{--}54$ meV and $2\Delta(\parallel\text{CuO}_2)=80\text{--}88$ meV. $2\Delta(\perp\text{CuO}_2)$ is in fairly good agreement with the result in Fig. 6(a) ($2\Delta\sim 50\text{--}60$ meV), synthesized under different conditions. $2\Delta(\parallel\text{CuO}_2)$ also agrees with those of Fig. 2(a) and Fig. 7(a). The ratio of gaps is $\Delta(\parallel\text{CuO}_2)/\Delta(\perp\text{CuO}_2)=1.5\text{--}1.8$. Since T_c is approximately 103 K, $2\Delta(\parallel\text{CuO}_2)/kT_c=9.0\text{--}9.9$, $2\Delta(\perp\text{CuO}_2)/kT_c=5.5\text{--}6.1$. Figure 8(b) shows the result of gap anisotropy measurements in the Bi-Sr-Ca-Cu-O 2:2:1:2 phase. The x-ray diffraction pattern of sample S-5 shows that the Bi-Sr-Ca-Cu-O 2:2:2:3 phase is mixed in the Bi-Sr-Ca-Cu-O 2:2:1:2 phase (ratio of 2:2:2:3 to 2:2:1:2 equals 1:3), though zero resistance is attained at $T=103$ K. Therefore, the energy gaps of the Bi-Sr-Ca-Cu-O 2:2:1:2 phase can be reasonably observed for sample S-5. The gap values in the Bi-Sr-Ca-Cu-O 2:2:1:2 phase are $2\Delta(\perp\text{CuO}_2)=38\text{--}40$ meV, $2\Delta(\parallel\text{CuO}_2)=68\text{--}70$ meV, $\Delta(\parallel\text{CuO}_2)/\Delta(\perp\text{CuO}_2)=1.7\text{--}1.8$ which agrees with that of the Bi-Sr-Ca-Cu-O 2:2:2:3 phase. The $2\Delta(\perp\text{CuO}_2)$ value is consistent with that of Lee *et al.*¹⁷ and Chen *et al.*¹⁸ The $2\Delta(\parallel\text{CuO}_2)$ value is almost the same as those of Fig. 1(a) and Fig. 5. These results confirm that the gap anisotropies in the Bi-Sr-Ca-Cu-O systems are larger than that of Y-Ba-Cu-O, where $\Delta(\parallel\text{CuO}_2)/\Delta(\perp\text{CuO}_2)=1.3\text{--}1.6$.^{19,20}

C. Gap measurements in the Bi-Sr-Cu-O system

Electron tunneling measurements in Bi-Sr-Cu-O draw less attention since T_c is low (7 K). However, it implies

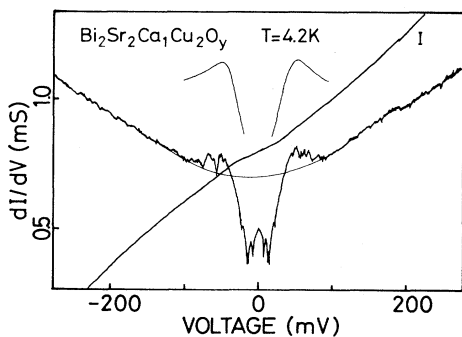


FIG. 5. The I - V and dI/dV - V curves for tunneling parallel to CuO_2 planes in the single-crystal sample S-2. 2Δ obtained from the interval of points, where the $(dI/dV)_s$ (raw data) and $(dI/dV)_n$ (narrow solid line) cross each other, is about 73 meV. The upper curve shows the difference between $(dI/dV)_s$ and $(dI/dV)_n$.

the key point in understanding why T_c 's are so different between Bi-Sr-Cu-O and Bi-Sr-Ca-Cu-O. To elucidate the difference of the pairing mechanisms between Bi-Sr-Ca-Cu-O and Ca-absent Bi-Sr-Cu-O, we have made tunneling measurements in this Ca-absent material. Two types of samples, S-6 ($T_c=8.0\text{--}6.5$ K) and S-7 ($T_c=11\text{--}7$ K), were used. Figure 9(a) shows the

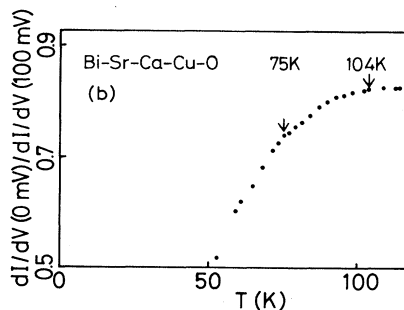
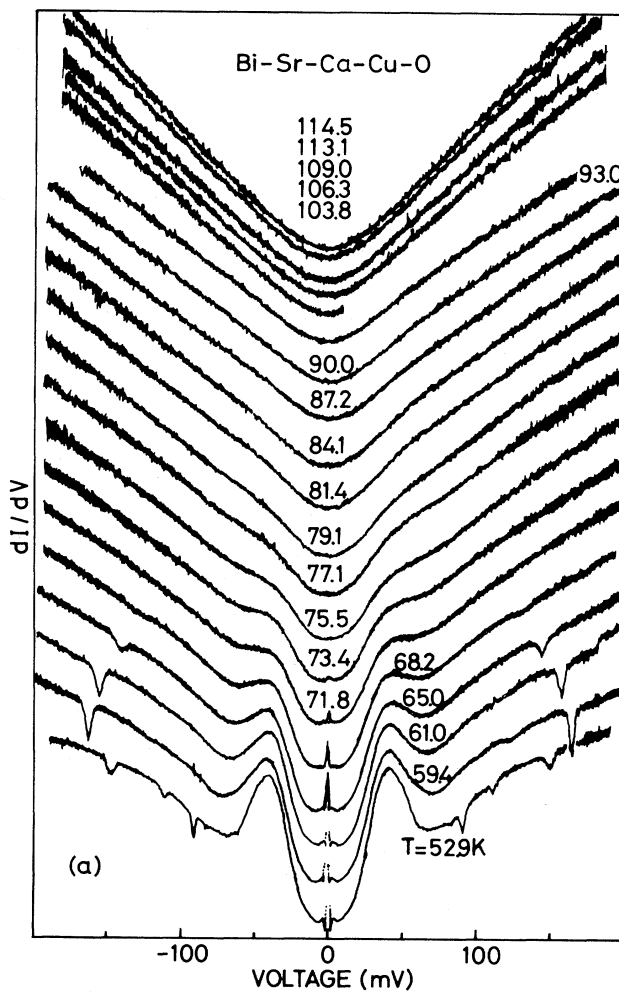


FIG. 6. (a) Temperature variation of dI/dV raw data for sample S-3. (b) Temperature variation of dI/dV at zero bias normalized by dI/dV at 100 mV. Data are taken from (a). Gap opening begins at $T=104$ K and 75 K. These correspond to each phase of Bi-Sr-Ca-Cu-O.

dI/dV - V curves from different tunnel junctions made from S-6 with Al sheets as counter electrodes. Since the present samples are more brittle than Ca-contained materials, high-quality point-contact tunnel junctions are difficult to obtain. However, the dI/dV curves are symmetric with respect to their zero biases. The upper curve

shows Josephson-like anomaly at zero bias. Tunnel resistances at the biases of 10 mV are about 0.7Ω for the upper curve and 15Ω for the lower curve. The gap opening begins at the same biases despite the large difference of tunnel resistances. This indicates the intrinsic feature of this material. The reductions of dI/dV (0 mV) are

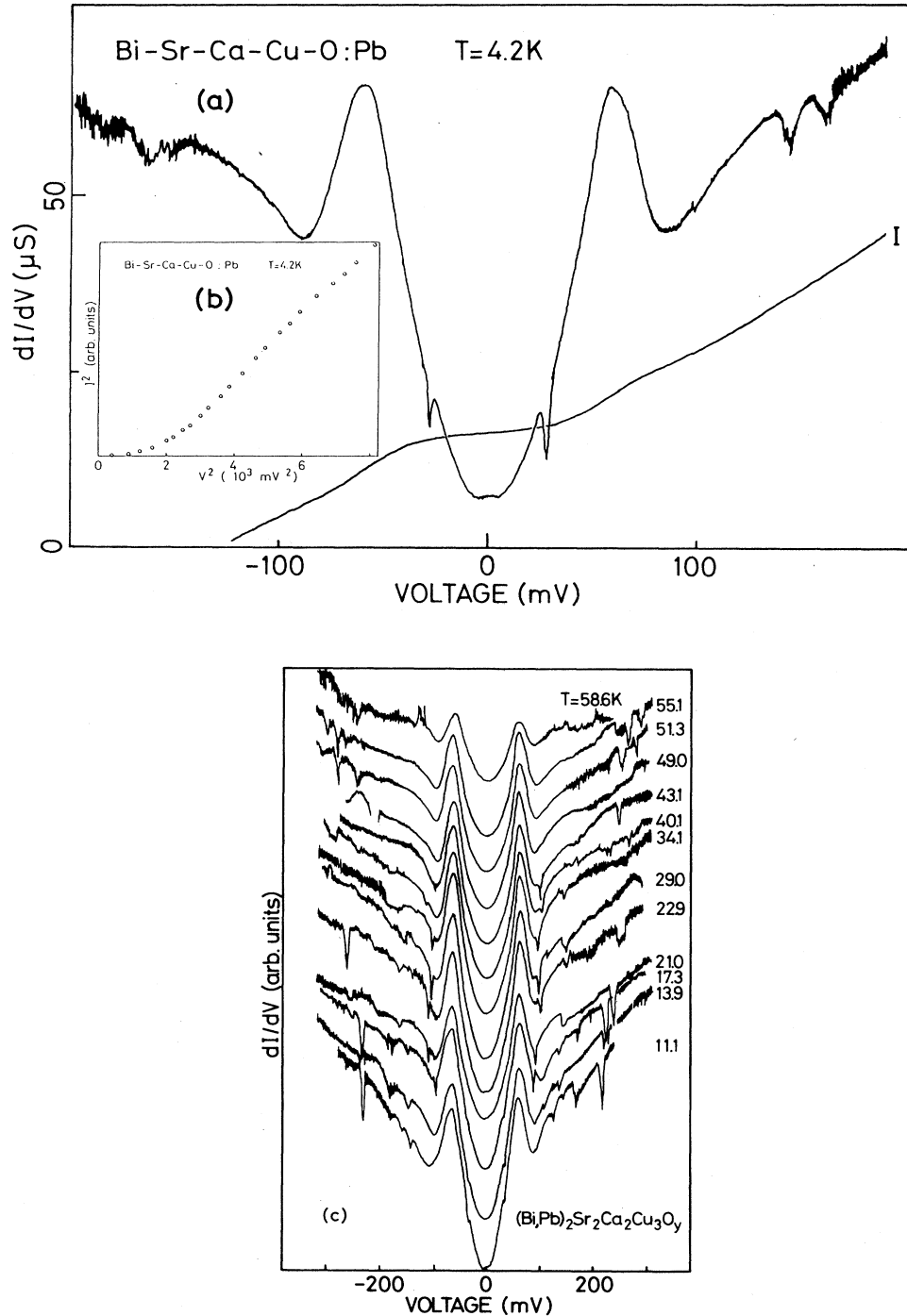


FIG. 7. (a) The I - V and dI/dV - V curves for Pb doped Bi-Sr-Ca-Cu-O 2:2:2:3 (sample S-4). (b) I^2 vs V^2 plot obtained from the I - V curve in (a). A straight line can be drawn between 3-6 (10^3 mV^2). From the extrapolated line to $I=0$, 2Δ is obtained as 85-87 meV. (c) Temperature variation of dI/dV raw data up to $T=58.6\text{K}$. The tunnel junction is identical with that of (a).

about 10% (the upper curve) and 14% (the lower curve) of their each peaks in dI/dV . These are not so drastic compared with the cases of Bi-Sr-Ca-Cu-O. This may be due to the large leakage current through the junctions, i.e., electron tunneling between nonsuperconducting materials. This will be suggested by the small superconducting volume fraction ($< 10\%$) of Bi-Sr-Cu-O. In the lower

curve, the gap value estimated from the bias at $(dI/dV)_s = (dI/dV)_n$ is 3.0–3.5 meV, which yields $2\Delta/kT_c = 5.4\text{--}6.2$ with a T_c of 6.5 K. Figure 9(b) shows the set of dI/dV - V curves for several tunnel junctions from sample *S-7* with Pt sheets. Tunnel resistances are 3 k Ω (the upper curve) and 133 Ω (the lower curve) near the gap edges. While the tunnel resistances are so

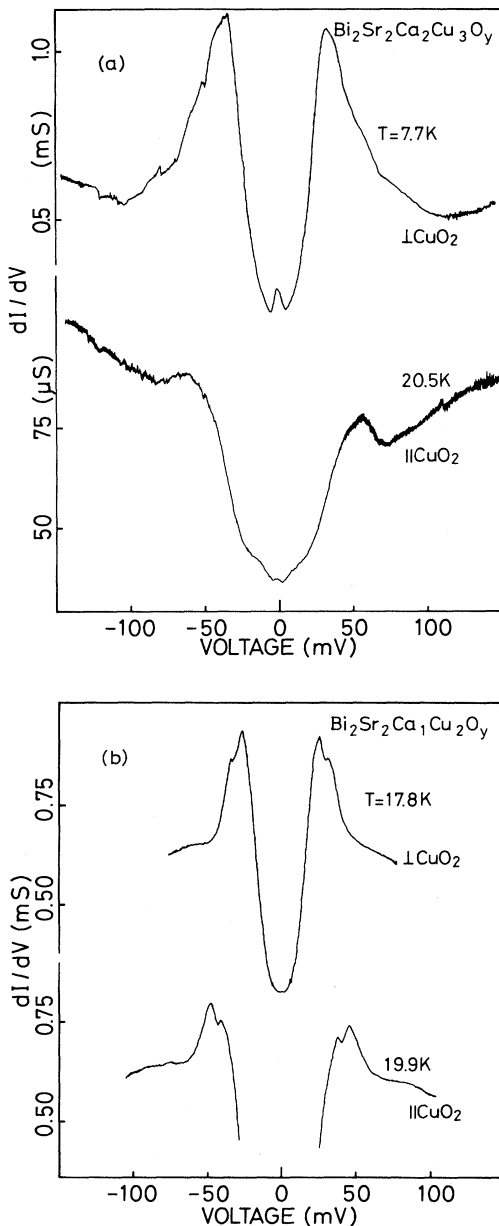


FIG. 8. (a) Gap anisotropy in Bi-Sr-Ca-Cu-O 2:2:2:3 phase of sample *S-5*. Electron tunneling parallel ($\parallel\text{CuO}_2$) and perpendicular ($\perp\text{CuO}_2$) to the CuO_2 planes. $2\Delta(\parallel\text{CuO}_2) = 80\text{--}88$ meV and $2\Delta(\perp\text{CuO}_2) = 49\text{--}54$ meV are obtained. The ratio of gaps is $\Delta(\parallel\text{CuO}_2)/\Delta(\perp\text{CuO}_2) = 1.5\text{--}1.8$. (b) Gap anisotropy in Bi-Sr-Ca-Cu-O 2:2:1:2 phase of sample *S-5*. $2\Delta(\parallel\text{CuO}_2) = 68\text{--}70$ meV. $2\Delta(\perp\text{CuO}_2) = 38\text{--}40$ meV. $\Delta(\parallel\text{CuO}_2)/\Delta(\perp\text{CuO}_2) = 1.7\text{--}1.8$.

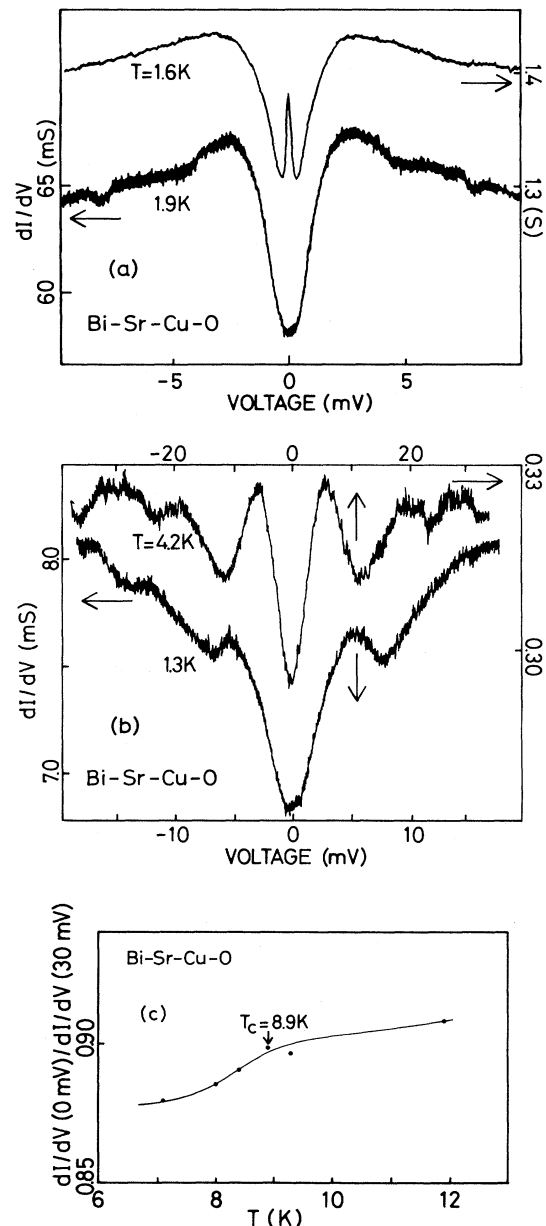


FIG. 9. (a) The dI/dV - V curves of $\text{Bi}_2\text{Sr}_2\text{Cu}_{1.3}\text{O}_y$ (sample *S-6*). Two curves are obtained from different tunnel junctions. $2\Delta = 3.0\text{--}3.5$ meV are obtained from the lower curve. (b) The dI/dV - V curves of $\text{Bi}_2\text{Sr}_2\text{Cu}_1\text{O}_y$ (sample *S-7*). Two curves are obtained from different tunnel junctions. $2\Delta = 5.0\text{--}5.7$ meV. (c) Temperature dependence of dI/dV at zero bias normalized by the dI/dV at 30 mV. This is obtained from the same tunnel junction which shows the lower curve in (b).

different (factor of 20) and the tunneling densities of states varies in their shapes, the bias positions of the peaks in dI/dV are almost the same. The gap values in these cases are 5.0–5.7 meV. Figure 9(c) presents the temperature dependence of dI/dV (0 mV) normalized by dI/dV (30 mV) in the upper curve of Fig. 9(b). A T_c of 8.9 K is obtained from the temperature that dI/dV (0 mV) begins to reduce. The ratio $2\Delta/kT_c$ of sample *S-7* is 6.5–7.4, and this is much larger than that of the BCS value.

V. DISCUSSIONS

As shown in Figs. 1(a), 2(a), 8(b), 9(a), the dI/dV curves of Bi-Sr-Ca-Cu-O and Bi-Sr-Cu-O are symmetric with respect to the Fermi level and flat with respect to bias voltage. These results suggest that the bias-dependent dI/dV curves outside the gap and asymmetric natures are not intrinsic for the tunneling density of states in the cuprates oxides. These can be attributed to the asymmetric potential barriers and/or low work functions of insulating layers in the tunnel junctions. However, the symmetric dI/dV curve with respect to the Fermi level and flatness against the bias have rarely been observed for La-Sr-Cu-O and Y-Ba-Cu-O.

The measurements on La-Sr-Cu-O yield $2\Delta/kT_c \sim 5$. There seems to be general agreement in the data for this value, which can be explained within the strong coupling regime extended from the BCS theory. In Y-Ba-Cu-O, $2\Delta/kT_c$ values are converged to 4–5 among almost all researchers. In the present paper we reported extremely large values of $2\Delta/kT_c$ in both phases of Bi-Sr-Ca-Cu-O and considerably large values in Bi-Sr-Cu-O systems. It should be emphasized that the data are reproducible.

Before discussing the origin of the large energy gaps in Bi-Sr-Ca-Cu-O and Bi-Sr-Cu-O, the possibilities of nonintrinsic energy gap structure should be considered. Recently, Barner and Ruggiero²¹ and Bentum *et al.*²² observed the tunneling characteristics for systems consisting of small isolated metal particles embedded between two tunneling electrodes. These data closely resemble the tunneling characteristics reported for the high- T_c superconductors. These data, however, are not originated from the intrinsic superconducting energy gap, but from the so-called charging effects related to the surface granularity of the materials. In this case, tunneling first begins to occur at $V = \pm e/2C$, where C is the capacitance of the particles. However, in our experiments, this is not likely since the gap values are quite reproducible by changing the contact pressure, i.e., capacitances of the tunnel junctions. Another possibility is that electron tunneling occurs between two superconducting regions within the sample [superconductor-insulator-superconductor (SIS) configuration]. This is also unlikely because we have sometimes observed the gap which seems to be that of the SIS configuration; it is broader in shape and has a Josephson-like zero-bias anomaly, but is almost twice as large as that which most frequently appeared.

It is difficult to understand why the present results on Bi-Sr-Ca-Cu-O and Bi-Sr-Cu-O give a much larger $2\Delta/kT_c$ than that of Y-Ba-Cu-O and La-Sr-Cu-O, where

the same CuO_2 planes are crucial for the superconductivity. Especially, it should be noted that Bi-Sr-Ca-Cu-O and Y-Ba-Cu-O have nearly the same T_c of about 100 K, whereas $2\Delta/kT_c$ values in Bi-Sr-Ca-Cu-O are more than 2 times larger than that of Y-Ba-Cu-O. It is known that the short coherence length of high- T_c oxides induces weakening of the gap value at the interface of the tunnel junction.²³ Assuming that pairing mechanisms are the same, the gap values are expected to be the same, since the coherence lengths of Y-Ba-Cu-O and Bi-Sr-Ca-Cu-O are short and of the same order of magnitude.

Vieira *et al.*²⁴ observed the distribution of superconducting energy gaps for Bi-Sr-Ca-Cu-O polycrystalline samples by STM with a Pt-Rh tip. Their tunnel resistances are about 10–100 M Ω , whereas in our experiments, they typically show about 10 k Ω . This means that tunnel current in our case possibly flows through the broad region of the sample surface. One of their main conclusions is the broad distribution of the energy gap. Most of their data ranging from 30 to 46 meV in 2Δ are determined by the energy separation between the maximum and the minimum in d^2I/dV^2 , and these values result in $2\Delta/kT_c = 4.5$ –6.5. The maximum value of their data was $2\Delta \approx 60$ meV which is somewhat smaller than our typical data of polycrystalline samples of the Bi-Sr-Ca-Cu-O 2:2:1:2 phase ($2\Delta = 68$ –76 meV). However, this coincides with our smaller gap obtained from the film measurements discussed in Sec. IV B.

The high resolution photoemission study of Bi-Sr-Ca-Cu-O 2:2:1:2 single crystals by Imer *et al.*²⁵ shows $2\Delta = 60 \pm 10$ meV. They observed unambiguously the low-lying quasiparticle excitation originating from the superconducting states. Their gap value was obtained by an analytic procedure where Δ was varied until a satisfactory agreement was obtained between the experimental data and the simple model for the superconducting density of states. This gap value yields $2\Delta/kT_c = 8 \pm 1.4$ within our results.

We will list the differences between Bi-Sr-Ca-Cu-O, Bi-Sr-Cu-O, La-Sr-Cu-O, and Y-Ba-Cu-O except for those with values of $2\Delta/kT_c$. One difference is found in the crystal structures; the former group consists of multiple layer structures, having CuO_2 and insulating Bi_2O_2 layers, while the latter consists of the stacking of CuO_2 layers. The difference may be reflected in the degree of anisotropies of H_{c2} and energy gaps with respect to CuO_2 planes.

Another difference between Bi-Sr-Ca-Cu-O and Y-Ba-Cu-O was clarified from the specific-heat measurements. Yuan *et al.*²⁶ obtained the jump of specific heat at T_c ($\Delta C/T_c$) in $\text{Bi}_1\text{Sr}_1\text{Ca}_1\text{Cu}_3\text{O}_y$ ($T_c = 80$ K) as 0.49 mJ/g.K², whereas 56–62 mJ/mol.K² was in Y-Ba-Cu-O.²⁷ This means that the electronic density of states near the Fermi level in Bi-Sr-Ca-Cu-O is much larger than that of Y-Ba-Cu-O, although both have the same T_c . This may be reflected in the large energy gaps in Bi-Sr-Ca-Cu-O.

Recently, Den and Akimitsu²⁸ pointed out that the hole carrier concentrations p in Bi-Sr-Ca-Cu-O and Bi-Sr-Cu-O are substantially in excess compared with those of La-Sr-Cu-O and Y-Ba-Cu-O. Excess p in the cu-

prates is known to suppress the T_c . An appropriate doping to control p makes T_c higher. For example, in the Bi-Sr-Ca-Cu-O 2:2:1:2 phase, substitution of Y on the Ca site raises T_c about 10 K at Y 30% mole ratios. Fein *et al.*²⁹ observed very large apparent gaps for $\text{La}_{1.77}\text{Sr}_{0.23}\text{CuO}_{4-y}$, and we also preliminarily observed very large gap structure (30–35 meV) taken as a peak-to-peak value in dI/dV for $\text{La}_{1.7}\text{Sr}_{0.3}\text{CuO}_4$ with T_c below 4 K. Both cases are within the excess hole region in the La-Sr-Cu-O system. Whether or not these excess hole concentration states enlarge the gap value is still under investigation.

There are no crystallographic differences between the samples of nominal compositions $\text{Bi}_2\text{Sr}_2\text{Cu}_{1.3}\text{O}_y$ (S-6) and $\text{Bi}_2\text{Sr}_2\text{Cu}_1\text{O}_y$ (S-7). Slight differences of T_c may be attributed to the difference of net p on the CuO_2 planes. The ratios $2\Delta/kT_c$ for Bi-Sr-Cu-O are much larger than those of conventional superconductors having almost the same T_c . For example, another low carrier density oxide superconductor $\text{BaPb}_{1-x}\text{Bi}_x\text{O}_3$ (Ba-Pb-Bi-O) has the same T_c (= 10 K) as Bi-Sr-Cu-O, and $2\Delta/kT_c \cong 3.5$ within the BCS value.^{30,31} In addition, the $2\Delta/kT_c$ of Bi-Sr-Cu-O has larger values than those of La-Sr-Cu-O and Y-Ba-Cu-O in spite of the lower T_c . Small $2\Delta/kT_c$ with small reduction of $(dI/dV)_s$ (0 mV) can explain that the material at the point contact region is different from the regular stoichiometry of the superconducting phase. However, large $2\Delta/kT_c$ and small reductions of $(dI/dV)_s$ (0 mV), like in these cases, are difficult to understand unless this is an intrinsic feature in this material.

We turn to consider the gap values in Bi-Sr-Ca-Cu-O on a basis of those in Bi-Sr-Cu-O. Why does the insertion of more CuO_2 planes drastically raise T_c and why does it enhance the $2\Delta/kT_c$ of 6–7 in Bi-Sr-Cu-O to 9–12 in Bi-Sr-Ca-Cu-O? One of the reasons is the increase of carrier concentration which contributes to the superconductivity as discussed in the case of Bi-Sr-Ca-Cu-O and Y-Ba-Cu-O. Why does this enhancement occur from Bi-Sr-Cu-O to Bi-Sr-Ca-Cu-O 2:2:1:2, and not occur from the Bi-Sr-Ca-Cu-O 2:2:1:2 phase to the Bi-Sr-Ca-Cu-O 2:2:2:3 phase?

The differences in $2\Delta/kT_c$ between Bi-Sr-Ca-Cu-O,

Bi-Sr-Cu-O, La-Sr-Cu-O, and Y-Ba-Cu-O should be carefully supported with further experimental evidence that the electronic properties in Bi-Sr-Ca-Cu-O and Bi-Sr-Cu-O systems are different from those of La-Sr-Cu-O and Y-Ba-Cu-O systems.

We finally briefly mention the structures observed at $V \cong 120$ –140 mV ($eV - \Delta \cong 80$ –120 meV) in the dI/dV curves as observed in Figs. 1, 2(a), 7(a), and 7(c). The anomaly of this bias region is also observed by Miyakawa *et al.*³² and Bulaevskii *et al.*³³ in a single crystal of Bi-Sr-Ca-Cu-O (Ref. 32) and $\text{EuBa}_2\text{Cu}_3\text{O}_y$,³³ respectively. This is possibly attributed to some kind of excitation corresponding to the superconductivity. Moreover, it is worthy to note that the effective exchange interaction in the cuprate oxides is on the order of 100 meV. Miyakawa *et al.*³² observed other complicated structures in the dI/dV curves of Bi-Sr-Ca-Cu-O single crystals and they attributed these structures to a multiphonon process.

VI. CONCLUSION

In summary, we observed reproducible large energy gaps in Bi-Sr-Cu-O and Bi-Sr-Ca-Cu-O systems: $2\Delta/kT_c$ are 5.4–7.4 for Bi-Sr-Cu-O polycrystals, 11.6–12.4 for Bi-Sr-Ca-Cu-O 2:2:1:2, 9.2–11.0, and 5.9–7.1 for Bi-Sr-Ca-Cu-O 2:2:2:3, and 9.6–11.0 for Bi-Sr-Ca-Cu-O 2:2:1:2 single crystals tunneling parallel to CuO_2 planes. Gap anisotropies are $\Delta(\parallel\text{CuO}_2)/\Delta(\perp\text{CuO}_2) = 1.5$ –1.8 for Bi-Sr-Ca-Cu-O 2:2:2:3, 1.7–1.8 for Bi-Sr-Ca-Cu-O 2:2:1:2, and $2\Delta/kT_c$ are 9.0–9.9 ($\parallel\text{CuO}_2$), 5.5–6.1 ($\perp\text{CuO}_2$) for Bi-Sr-Ca-Cu-O 2:2:2:3 film. The gap values are larger than those of BCS but quite reproducible from sample to sample even though the synthesis conditions are different.

ACKNOWLEDGMENTS

We thank Dr. T. Nakada and Professor A. Kunioka for kindly supplying the Pb-doped Bi-Sr-Ca-Cu-O sputtered films. This work was partially supported by a Grant-in-Aid for Scientific Research on Priority Areas "Mechanism of Superconductivity."

*Present address: Faculty of Integrated Arts and Sciences, Hiroshima University, Hiroshima 730, Japan.

¹See, for example, *Novel Superconductivity*, edited by S. A. Wolf and V. Z. Kresin (Plenum, New York, 1987).

²M. C. Gallagher, J. G. Adler, J. Jung, and J. P. Franck, *Phys. Rev. B* **37**, 7846 (1988).

³K. W. Ng, S. Pan, A. L. de Lozanne, A. J. Panson and J. Talvacchio, Proceedings of the 18th International Conference on Low Temperature Physics, Kyoto, 1987 [*Jpn. J. Appl. Phys.* **26**, Suppl. **26-3**, 993 (1987)].

⁴T. Ekino, J. Akimitsu, M. Sato, and S. Hosoya, *Solid State Commun.* **62**, 535 (1987).

⁵T. Ekino and J. Akimitsu, *Jpn. J. Appl. Phys.* **26**, L452 (1987).

⁶Y. Iye *et al.* (private communication).

⁷H. Maeda, Y. Tanaka, M. Fukutomi, and T. Asano, *Jpn. J. Appl. Phys.* **27**, L209 (1988).

⁸M. Kazusawa, K. Takahashi, T. Nakada, and A. Kunioka, Report No. CPM-88-50, 1988, p. 101.

⁹C. Michel, M. Hervieu, M. Borel, A. Gradin, F. Deslandes, J. Prorost and B. Raveau, *Z. Phys. B* **68**, 421 (1987).

¹⁰J. Akimitsu, A. Yamazaki, H. Sawa, and H. Fujiki, *Jpn. J. Appl. Phys.* **26**, L2080 (1987).

¹¹T. Ekino, J. Akimitsu, Y. Matsuda, and M. Sato, *Solid State Commun.* **63**, 41 (1987).

¹²*Progress in Low Temperature Physics*, edited by C. J. Gorter (North-Holland, Amsterdam, 1964).

¹³M. E. Hawley, K. E. Gray, B. D. Terris, H. H. Wang, K. D. Carlson, and J. M. Williams, *Phys. Rev. Lett.* **57**, 629 (1986).

¹⁴M. E. Hawley, K. E. Gray, D. W. Capone, and D. G. Hinks, *Phys. Rev. B* **35**, 7224 (1987).

¹⁵R. C. Dynes, V. Narayanamurti, and J. P. Garno, *Phys. Rev. Lett.* **41**, 1509 (1978).

- ¹⁶M. D. Kirk, C. B. Eom, B. Oh, S. R. Spielman, M. R. Beasley, A. Kapitulnik, T. H. Geballe, and C. F. Quate, *Appl. Phys. Lett.* **52**, 2071 (1988).
- ¹⁷M. Lee, D. B. Mitzi, A. Kapitulnik, and M. R. Beasley, *Phys. Rev. B* **39**, 801 (1989).
- ¹⁸Y. Chen, H. Tao, S. Zhao, Y. Yan, and Q. Yang, *Modern Phys. Lett.* **2**, 903 (1988).
- ¹⁹J. S. Tsai, I. Takeuchi, J. Fujita, T. Yoshitake, S. Miura, S. Tanaka, T. Terashima, Y. Bando, K. Iijima, and K. Yamamoto, *Fifth International Workshop on Future Electron Devices and High-Temperature Superconducting Electron Devices*, Miyagi-Zao, 1988 (unpublished).
- ²⁰T. Ekino and J. Akimitsu (unpublished).
- ²¹J. B. Barner and S. T. Ruggiero, *Phys. Rev. Lett.* **59**, 807 (1987).
- ²²P. J. M. van Bentum, R. T. M. Smokes, and H. van Kempen, *Phys. Rev. Lett.* **60**, 2543 (1988).
- ²³G. Deutscher and K. A. Muller, *Phys. Rev. Lett.* **59**, 1745 (1987).
- ²⁴S. Vieira, M. A. Ramos, M. Vallet-Regi, and J. M. Gonzalezt-Calbet, *Phys. Rev. B* **38**, 9295 (1988).
- ²⁵J. M. Imer, F. Patthey, B. Darel, W. D. Schneider, Y. Baer, Y. Petroff, and A. Zettl, *Phys. Rev. Lett.* **62**, 336 (1989).
- ²⁶S. L. Yuan, J. W. Li, W. Wang, Q. Z. Ran, G. G. Zheng, W. Y. Guan, and J. Q. Zheng, *Mod. Phys. Lett.* **2**, 885 (1988).
- ²⁷M. Ishikawa, Y. Nakazawa, T. Takabatake, A. Kishi, R. Kato, and A. Maesono, *Physica* **153C-155C**, 1089 (1988).
- ²⁸T. Den and J. Akimitsu, *Jpn. J. Appl. Phys.* **28** (1989).
- ²⁹A. P. Fein, J. R. Kirtley, and M. W. Shafer, *Phys. Rev. B* **37**, 9738 (1988).
- ³⁰B. Batlogg, J. P. Remeika, R. C. Dynes, H. Barz, A. S. Cooper, and J. P. Garno, in *Superconductivity in d- and f-Band Metals*, edited by W. Buckel and W. Weber (Kernforschungszentrum, Karlsruhe, 1982).
- ³¹T. Ekino and J. Akimitsu, *J. Phys. Soc. Jpn.* **58**, 2135 (1989).
- ³²N. Miyakawa, D. Shimada, T. Kido, and N. Tsuda, *J. Phys. Soc. Jpn.* **58**, L1141 (1989).
- ³³L. N. Bulaevskii, O. V. Dolgov, I. P. Kazakov, S. N. Maksimovskii, M. O. Ptitsyn, V. A. Stepanov, and S. I. Vedeneev, *Superconduct. Sci. and Technol.* **1**, 205 (1988).